BSc Thesis
Applied Mathematics & Applied Physics

Calculation of 2D spin-galvanic effects in diffusive metals

Danny Knol

Supervisors:
B. J. Geurts
A. Brinkman
T. H. Kokkeler

June, 2024

Department of Applied Mathematics
Faculty of Electrical Engineering,
Mathematics and Computer Science

Department of Applied Physics
Faculty of Science and Technology

UNIVERSITY OF TWENTE.

Preface

This article was written in the context of my Bachelor's Assignment.

I would like to thank my supervisors for properly guiding me through the difficult process of doing actual research for the first time. Bernard Geurts for giving me advice about various numerical methods, Alexander Brinkman for giving feedback about the explanations for the physical background and of course Tim Kokkeler for helping me (almost) every day with all sorts of problems that I encountered as well as coming up with many suggestion for my work during the past nine weeks.

I also want to mention my fellow students with whom I have exchanged ideas about our projects for their ideas and also my parents, little sisters and my housemates for making sure that I also had a nice break from this project from time to time.

Calculation of 2D spin-galvanic effects in diffusive metals

Danny Knol*

June, 2024

Abstract

In this thesis, the spin-galvanic effect in a 2D diffusive metal with spin-charge coupling in the steady state is calculated. The calculations are done by using central differencing and the ghost cell method on the Usadel equation on a numerical grid. We find that the voltage across the system is linearly dependent on the time derivative of the applied magnetic field and the strength of the spin-galvanic effect.

Keywords: spin-charge coupling, 2D Usadel equation, spin-galvanic effect

Contents

*Email: d.knol@student.utwente.nl

List of Figures

List of Tables

1 Introduction

In our society, the amount of data that is generated keeps increasing, so we need ever more data storage as well [1]. Moore's Law states that the amount of transistors that fit on a circuit board doubles every year. Recently however it was predicted that the law is not going to hold anymore in the near future [2]. The techniques for reducing the transistors in size are limited. Making better storage devices can be achieved by using electronics that make use of different quantum effects and if the devices made are on such a small scale, quantum effects will be present anyway so it makes sense to look for ways to make use of them.

Some devices that manipulate electron spin to their advantage are called spintronic devices or spintronics [3]. Improving storage capacity is not the only goal of the development of spintronics. The devices also improve computation power of computers and ways to increase efficiency are being researched [4], so the spintronic devices can help reduce the amount of energy consumption. For normal electrical current, a voltage is needed. When we are considering spin transport, an electrical current is not required so there is less dissipation, which means that some energy can be saved.

A possibility is to produce the devices with materials that have spin-orbit coupling. Spin-orbit coupling is in our case the effect that electron spin is coupled to a magnetic field [5] and electrons with spin up behave differently in a magnetic field than electrons with spin down. The specific type of spin-orbit coupling that we are going to consider is Rashba spin-orbit coupling [6].

To make the spintronic devices better, we need to understand more about the materials with spin-orbit coupling. The electron transport behaviour in the materials is modeled by the Usadel equation [7] and recently, a newly developed form of this equation was published [8]. The Usadel equation is a diffusion equation that also incorporates different quantum effects and describes transport in junctions on a mesoscopic level in these materials. We can use a diffusion equation to describe these materials, because in practice, due to manufacturing errors, the materials are almost always diffuse. It is useful to look at a numerical solution of the equation to understand the materials better.

The spintronics are not the only relevant applications of the problem that we are considering. A long term goal is to add superconductivity to the problem. Then it is possible to make predictions and people can do the experiment and then we can compare the outcome of the experiments to the predictions that we have made numerically. Before we consider the effects of superconductivity, we have to properly model the system in normal state first.

In this thesis, the systems that we will look at are 2D diffusive metals with Rashba spin-orbit coupling. We are interested in calculating the steady state solutions, specifically the voltage in the steady state that is caused by the application of a magnetic field is considered. The spin-galvanic effect plays an important role [9].

To this end, we will first elaborate the physical origins of the spin-galvanic effect. Then we look at numerical implementation of diffusion and we explain how we can add the spin-galvanic effect to the numerical diffusion. Lastly we show the calculations that we have done with the implemented model. We found that a gradient in the electron density is formed in the steady state that is perpendicular to the direction that the magnetic field is pointing in. We also found that the voltage increases linearly with both the strength of the magnetic field and the strength of the spin-orbit coupling.

2 Usadel equations for spin-galvanic effects

2.1 Usadel in normal state

To motivate the use of the Usadel equation, we will look at where the equation actually comes from. We will consider three key parts relating to the Usadel equation.

The systems that we are considering are all diffusive metals. To describe the different quantum effects that occur in these systems, we can not make use of pure classical methods. The simple reason is that classical methods do not consider spin-orbit coupling at all, while spin-orbit coupling is what all the effects we are interested in causes. To incorporate spin-orbit coupling, we need to look at the other end of the spectrum, namely quantum methods. Pure quantum methods are however not ideal to work with. The systems that we are interested in are too large and have too many impurities.

We see that we need some combination of classical and quantum methods to be able to describe the systems that we are interested in. The methods that have been developed for this problem are called quasiclassical methods [10] and we will be making use of the results of the quasiclassical methods. To use these methods we have to assume that the Fermi level is not too close to the band gap.

Impurities are a common occurrence in any material, because producing a perfect material is almost impossible, especially if the materials are mass produced. Therefore using systems that are not ballistic, so systems that have scattering, is a good approximation.

The equation that we can use to describe the systems that we are looking at is called the Usadel equation. The Usadel equation is a second order non-linear equation. We are interested in a situation where superconductivity is not involved and the absence of superconductivity greatly simplifies the Usadel equation. The equation becomes linear, which makes the equation become a lot easier to work with.

2.2 Explanation of spin-galvanic effect

The spin galvanic effect is an effect where a spin accumulation causes an electrical current to flow. We will first explain in 1D how the effect works and then an extension to 2D will be made.

To explain the spin-galvanic effect, we will make use of an example Hamiltonian. This is a very specific example that produces nice figures that make it easier to interpret the effect.

The Hamiltonian is given by

$$\beta k^4 + \frac{\hbar^2 k^2}{2m} + \gamma k_x \sigma_y - \sigma_y B \tag{1}$$

We can look at the expression in matrix form, since the spin Pauli matrix for y is $\begin{pmatrix} 0 & -i \\ i & 0 \end{pmatrix}$ [11], so the Hamiltonian can be written as

$$\beta k^4 \begin{pmatrix} 1 & 0 \\ 0 & 1 \end{pmatrix} + \frac{\hbar^2 k^2}{2m} \begin{pmatrix} 1 & 0 \\ 0 & 1 \end{pmatrix} + \gamma k_x \begin{pmatrix} 0 & -i \\ i & 0 \end{pmatrix} - B \begin{pmatrix} 0 & -i \\ i & 0 \end{pmatrix} \tag{2}$$

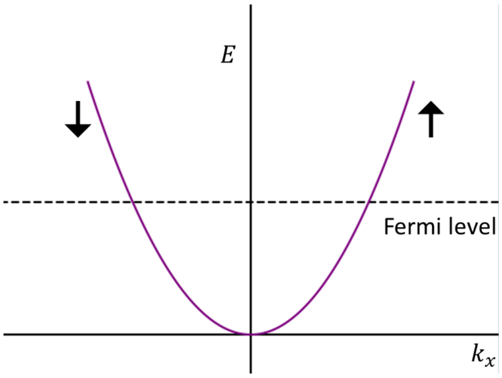

FIGURE 1: Available energy states depending on momentum for electrons with spin up and spin down

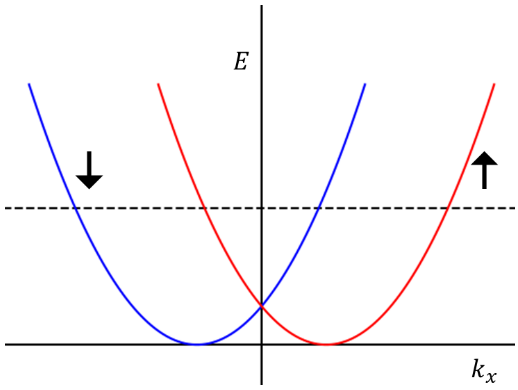

FIGURE 2: Available energy states for electrons with spin-orbit coupling. The dispersions for pin up and spin down are now separated

In a normal material, the galvanic coefficient γ is zero. Without a magnetic field $\boldsymbol{B}$, the only term that is left is the kinetic energy term $\beta k^4 + k^2/2m$, which means that the Hamiltonian is simply $\beta k^4 + \hbar^2 k^2/2m$ times the identity matrix $\mathbf{1}$.

The eigenvalues of this matrix are immediately read from the diagonals and are therefore twice $\beta k^4 + \hbar^2 k^2/2m$. One of the eigenvalues belongs to the electrons with spin up and the other eigenvalue belongs to the electrons with spin down. Since the eigenvalues are the same, the resulting dispersions are identical.

In figure 1, the situation without spin-orbit coupling and an external magnetic field is shown. The parabola for electrons with spin up overlaps with the parabola for electrons with spin down. The states up until the Fermi level are filled with electrons and since the Fermi level is the same for both spin up and spin down, nothing particularly interesting happens.

The materials that we are looking at have spin-orbit coupling, which means that γ in equation (2) is not zero. The Hamiltonian in that case is

$$\beta k^4 + \frac{\hbar^2 k^2}{2m} \begin{pmatrix} 1 & 0 \\ 0 & 1 \end{pmatrix} + \gamma k_x \begin{pmatrix} 0 & -i \\ i & 0 \end{pmatrix} \tag{3}$$

The eigenvalues of the matrix can be calculated and the result is that the eigenvalues are

$$\beta k^4 + \frac{\hbar^2 k^2}{2m} \pm \gamma k_x \tag{4}$$

Notice that now the two eigenvalues are not the same anymore for spin up and spin down. In figure 2, the dispersions for electrons with spin up and spin down do not overlap anymore.

Now we will add the magnetic field as well, implying that the magnetic field $\boldsymbol{B}$ in equation (2) is also not zero. The Hamiltonian can be written as

$$\begin{pmatrix} \beta k^4 + \frac{\hbar^2 k^2}{2m} & -i(\gamma k_x - \boldsymbol{B}) \\ i(\gamma k_x - \boldsymbol{B}) & \beta k^4 + \frac{\hbar^2 k^2}{2m} \end{pmatrix}$$

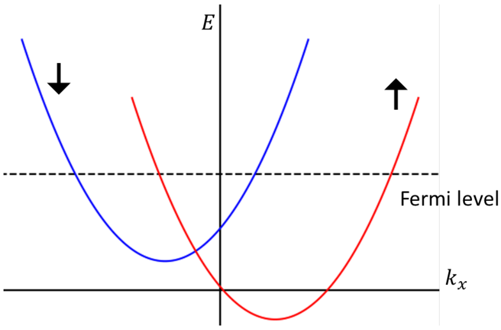

FIGURE 3: Available states for electrons with spin-orbit coupling in the presence of a magnetic field. The dispersions for spin down and spin up are shifted upwards and downwards respectively

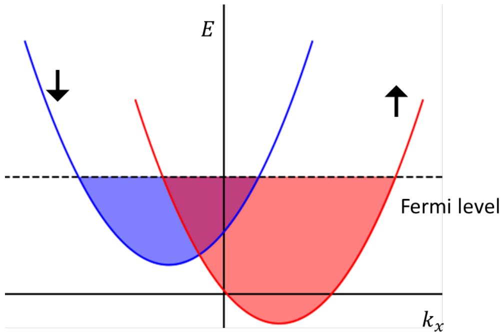

FIGURE 4: States occupied by electrons with spin-orbit coupling in the presence of a magnetic field. There are more occupied states for spin up than for spin down

We can calculate the eigenvalues again , which results in

$$\beta k^4 + \frac{\hbar^2 k^2}{2m} \pm (\gamma k_x - B) \tag{5}$$

as the eigenvalues of the Hamiltonian.

The magnetic field added a term that is independent of k_x, which means that a constant term has been added to the eigenvalues. This constant term is not the same for spin up and spin down. When we add an external magnetic field, the dispersion of one of the two types of electrons will shift up while the other dispersion will move down a bit, see figure 3.

In figure 4 the amount of electrons is visualised There are more electrons with spin down than electrons with spin up.

The dispersion of the electrons with spin up is moved towards the positive k. The dispersions are not perfectly parabolic, so the group velocity for positive k is not the same as the group velocity for negative k. This implies that there is electric current flowing.

A similar explanation can be used to explain the 2D version.

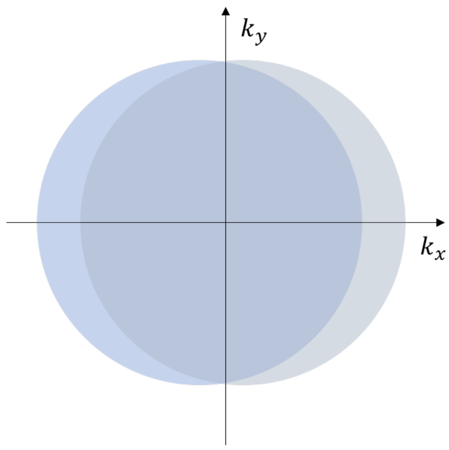

FIGURE 5: The two areas representing the available states for spin up and spin down are separated in 2D

In 2D, the available states form an area in k space. From figure 5 we can see that electrons with spin up have a different group velocity compared to the electrons with spin down. This difference in group velocity will cause a current to flow.

The consequence of the effect can be summarised in the following figure 6. Since we have more electrons moving in one direction than electrons moving in the opposite direction, we expect that a current must flow.

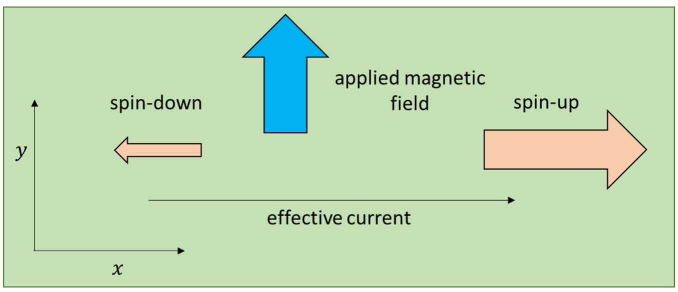

FIGURE 6: Applying a magnetic field to a material that has spin-orbit coupling causes a current to flow

2.3 Mathematical model

The calculations that we are going to do are based on mathematical models. In this section, we will present the bulk equations, boundary and initial conditions. The individual terms of the equations and the part of the physical system that they describe will also be explained.

2.3.1 Bulk equations

We effectively have four different equations, namely one for μ, S^x, S^y and S^z. Important to note is that S^c indicates the spin in direction c and that γ is a 3×3 tensor.

$$D\nabla^2\mu = \partial_t\mu + \gamma_{kl}\partial_k S^l \tag{6}$$

This equation is very straightforward. The term with the derivative with respect to t is the diffusion term. The terms with the derivative with respect to S is the term that corresponds to the spin-galvanic effect and contributes to the effect as we have described in the previous section. We are looking at 2D materials, so we have to sum over $k = x, y$ and the spin can be in direction x, y or z, so we have to sum over $l = x, y, z$.

$$D\nabla^2 S^c = \partial_t S^c + \frac{1}{\tau_{SO}}S^c + \chi\dot{B}^c + \alpha(\vec{h} \times \vec{S})^c + \gamma_{kc}\partial_k\mu \tag{7}$$

The equations that describe the spins have slightly more terms and are slightly more complicated. In equation (7), we look at the spin in direction c. Again, the term with the derivative with respect to t is the diffusion term and the term with γ is the term that induces the spin-galvanic effect. We have to sum over $k = x, y$.

Then we have the term with τ_{SO}. This is the spin relaxation term. Spin relaxation has multiple causes, namely scattering and precession caused by a small internal magnetic field.

The term $\chi\dot{B}$ represents the external magnetic field. We will look at the case that the time derivative of B is constant.

The term $\alpha(\vec{h} \times \vec{S})^c$ will be zero in the systems that we are interested in.

In addition to the bulk equations we have the equation for the current.

$$j_k = D\partial_k\mu + \gamma_{kl}S^l \tag{8}$$

Similarly, we have the equation for the spin current.

$$j_k^c = D\partial_k S^c + \gamma_{kc}\mu \tag{9}$$

2.3.2 Boundary conditions

The boundary conditions for both μ and all the three spins are that the corresponding currents must be zero in the direction of the edge. Intuitively we can say that the current is not allowed to leave the system at the edges.

In mathematical terms, the boundary conditions are given by

$$\begin{aligned} n_k j_k &= 0 \\ n_k j_k^c &= 0 \end{aligned} \tag{10}$$

2.3.3 Initial conditions

Since we are dealing with differential equations, we must provide initial conditions for the solutions. We will simply consider a general initial condition given by some function $f(x, y)$. The reason for the choice of any function is that we are interested in the steady state solution. The initial condition does not influence the final outcome, so the initial condition function can be anything.

2.3.4 Dimensionless units

For the discretization of these equations, we want to work with dimensionless units. We will first consider the equation for μ, which is equation (6).

We arbitrarily choose the length in the x- or y-direction of the system L as the characteristic length and we define

$$\begin{aligned} \tilde{x} &= \frac{x}{L} \\ \tilde{y} &= \frac{y}{L} \end{aligned} \tag{11}$$

as dimensionless variables. Then we can write

$$\frac{\partial}{\partial x} = \frac{\partial \tilde{x}}{\partial x}\frac{\partial}{\partial \tilde{x}} = \frac{1}{L}\frac{\partial}{\partial \tilde{x}} \tag{12}$$

Similarly,

$$\frac{\partial}{\partial y} = \frac{1}{L}\frac{\partial}{\partial \tilde{y}} \tag{13}$$

We can substitute x and y in equation (6) with $\tilde{x}$ and $\tilde{y}$, which gives us

$$D\frac{1}{L^2}\frac{\partial^2}{\partial \tilde{x}^2}\mu + D\frac{1}{L^2}\frac{\partial^2}{\partial \tilde{y}^2}\mu = \frac{\partial}{\partial t}\mu + \gamma_{xl}\frac{\partial}{\partial x}S^l + \gamma_{yl}\frac{\partial}{\partial y}S^l \tag{14}$$

Now that we have modified the left hand side of the equation, we need to do the same for the right hand side of the equation.

We want to write

$$\frac{\partial}{\partial t} = \frac{\partial \tilde{t}}{\partial t}\frac{\partial}{\partial \tilde{t}} \tag{15}$$

and we need to ensure that the units on both sides of the equation are identical. We can see that the left hand side consists of terms in D/L^2, so we conclude that

$$\frac{\partial \tilde{t}}{\partial t} = \frac{D}{L^2} \tag{16}$$

With this result we define the dimensionless variable

$$\tilde{t} = \frac{t}{t_D} \tag{17}$$

where $t_D = L^2/D$.
t_D is the characteristic diffusion time of the system and indicates how long it takes for the diffusion to have reached the entire system.

We have seen that a spatial derivative will have an extra $1/L$. This means that we can make the term with γ_{kl} dimensionless by defining

$$\tilde{\gamma}_{kl} = \frac{\gamma_{kl}}{L/D} \tag{18}$$

The dimensionless version of equation (6) is then

$$\frac{\partial^2}{\partial \tilde{x}^2}\mu + \frac{\partial^2}{\partial \tilde{y}^2}\mu = \frac{\partial}{\partial \tilde{t}}\mu + \tilde{\gamma}_{xl}\frac{\partial}{\partial x}S^l + \tilde{\gamma}_{yl}\frac{\partial}{\partial y}S^l \tag{19}$$

We also have to make the equation for S^c, equation (7), dimensionless. We can reuse the derivation that we have done in the equation for μ. Putting $\tilde{x}$, $\tilde{y}$, $\tilde{t}$ and $\tilde{\gamma}_{kl}$ in equation (7) gives

$$\frac{D}{L^2}\frac{\partial^2}{\partial \tilde{x}^2}S^c + \frac{D}{L^2}\frac{\partial^2}{\partial \tilde{y}^2}S^c = \frac{D}{L^2}\frac{\partial}{\partial \tilde{t}}S^c + \frac{D}{L^2}\tilde{\gamma}_{xc}\frac{\partial}{\partial x}\mu + \frac{D}{L^2}\tilde{\gamma}_{yc}\frac{\partial}{\partial y}\mu + \frac{1}{\tau_{SO}}S^c + \chi\dot{B} + \alpha(\vec{h}\times\vec{S})^c \tag{20}$$

To make the remaining terms of equation (20) dimensionless, we can make the following definitions:

$$\begin{aligned} \tilde{\tau}_{SO} &= \frac{L^2}{D}\tau_{SO} \\ \tilde{\chi} &= \frac{L^2}{D}\chi \\ \tilde{\alpha} &= \frac{L^2}{D}\alpha \end{aligned} \tag{21}$$

Substituting these in equation (20) gives

$$\frac{D}{L^2}\frac{\partial^2}{\partial \tilde{x}^2}S^c + \frac{D}{L^2}\frac{\partial^2}{\partial \tilde{y}^2}S^c = \frac{D}{L^2}\frac{\partial}{\partial \tilde{t}}S^c + \frac{D}{L^2}\tilde{\gamma}_{xc}\frac{\partial}{\partial x}\mu + \frac{D}{L^2}\tilde{\gamma}_{yc}\frac{\partial}{\partial y}\mu + \frac{D}{L^2}\frac{1}{\tilde{\tau}_{SO}}S^c + \frac{D}{L^2}\tilde{\chi}\dot{B} + \frac{D}{L^2}\tilde{\alpha}(\vec{h}\times\vec{S})^c \tag{22}$$

or

$$\frac{\partial^2}{\partial \tilde{x}^2}S^c + \frac{\partial^2}{\partial \tilde{y}^2}S^c = \frac{\partial}{\partial \tilde{t}}S^c + \tilde{\gamma}_{xc}\frac{\partial}{\partial x}\mu + \tilde{\gamma}_{yc}\frac{\partial}{\partial y}\mu + \frac{1}{\tilde{\tau}_{SO}}S^c + \tilde{\chi}\dot{B} + \tilde{\alpha}(\vec{h}\times\vec{S})^c \tag{23}$$

which is then our dimensionless version of equation (7).

In the following sections, we will be working with equations (19) and (23). For convenience we will write $\tilde{x}$ as x, and do the same for the other dimensionless variables.

3 Spatial discretization of diffusion core

In this section, we will discuss the discretization of the basic diffusion and we will show that the expected physical properties of diffusion are also present in the implementation. The discretizations are based on [12].

The diffusion equation for some quantity u is given by equation (24).

$$\nabla^2 u = \partial_t u \tag{24}$$

For the discretization in time, we have used the simple discretization as follows:

$$\partial_t u \approx \frac{U^{n+1} - U^n}{\Delta t} \tag{25}$$

where U is the discretized quantity, the index n denotes the time step and Δt is the difference in time between time step n and $n+1$.

3.1 Boundary conditions

For basic diffusion, the condition at the edges of the material is that the quantity is not allowed to leave the material. Mathematically, this can be described by

$$n_k \partial_k u = 0 \tag{26}$$

3.2 1D system

3.2.1 Discretization

Before we study the 2D case, we will create a model for 1D first. The numerical grid that we have used for the spatial discretization in 1D can be found in figure 7 along with the definitions of the indices and the directions.

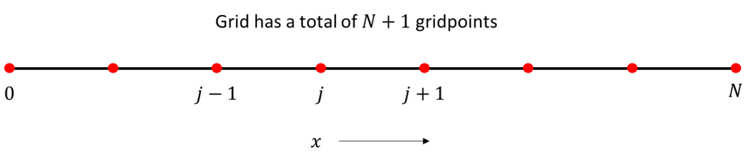

FIGURE 7: The 1D grid, indicating the indices that are used and the positive x-direction

Now that we have the grid, we can define the discretization

$$\nabla^2 u \approx \frac{U_{j+1} - 2U_j + U_{j-1}}{(\Delta x)^2} \tag{27}$$

Combining the discretizations for time and space gives us the following scheme that we can use for the bulk of the grid points. For simplicity, we introduce the notation $\nu = \Delta t/(\Delta x)^2$

$$U_j^{n+1} = (1 - 2\nu)U_j^n + \nu(U_{j+1} + U_{j-1}) \tag{28}$$

At the edges, equation (28) can not be used as it is. We can use the ghost-cell method to keep the second order accuracy and for that, the boundary conditions can be used to derive what the non-existing grid points are in terms of the other grid points.

Since we are looking at 1D, we have that $\partial_x u = 0$ for both edges. We will use central differencing for the discretization.

$$\frac{U_1 - U_{-1}}{2\Delta x} = 0 \tag{29}$$

from which we can conclude that $U_{-1} = U_1$. The grid point -1 is part of the aforementioned ghost cell method and does not exist on the grid that describes our system. That is why we have to find a way to eliminate U_{-1} from the numerical scheme. Similarly, we can derive that for the right edge that $U_{N+1} = U_{N-1}$. This time the grid point $N + 1$ does not exist on our grid.

The expressions for U_{-1} and U_{N+1} can then be substituted in equation (28) to get the scheme for the edges.

3.2.2 Conservation

An important property of diffusion is that the total amount of the quantity must be the same at each time step. We can verify that this property holds for the numerical scheme described above.

To be more precise, conservation of U means that

$$\frac{1}{2}U_0^{n+1} + \sum_{j=1}^{N-1} U_j^{n+1} + \frac{1}{2}U_N^{n+1} = \frac{1}{2}U_0^n + \sum_{j=1}^{N-1} U_j^n + \frac{1}{2}U_N^n \tag{30}$$

must hold.

Since every U_j^n is defined on a grid point, but every grid point governs half of the grid spaces between itself and its neighbours, see figure 8, we have to be careful with the end points.

The end points only contribute half of what the interior points contribute to the system. This means that

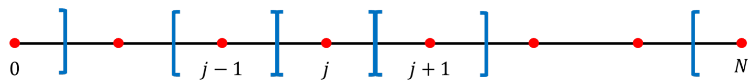

FIGURE 8: The grid points at the edge describe half of what an interior grid point describes of the system

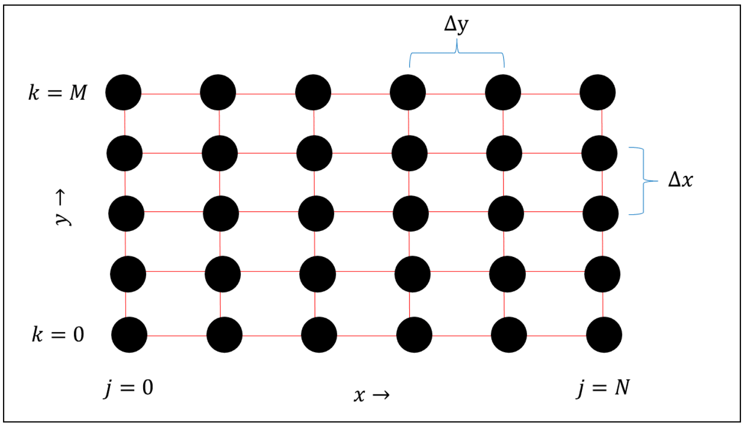

FIGURE 9: Representation of the 2D grid and the indices that are used for each grid point

We start the derivation by substituting equations (28) and the expression for the edges in the left hand side of equation (30). The resulting expression can be simplified all the way until the right hand side of equation (30) is recovered.

$$
\begin{aligned}
&\frac{1}{2}U_0^{n+1} + \sum_{j=1}^{N-1} U_j^{n+1} + \frac{1}{2}U_N^{n+1} \\
=&\frac{1}{2}(1-2\nu)U_0^n + \nu U_1^n + \sum_{j=1}^{N-1}[(1-2\nu)U_j^n + \nu(U_{j+1}^n + U_{j-1}^n)] + \frac{1}{2}(1-2\nu)U_N^n + \nu U_{N-1}^n \\
=&\frac{1}{2}U_0^n - \nu U_0^n + \nu U_1^n + \sum_{j=1}^{N-1} U_j^n - 2\nu \sum_{j=1}^{N-1} U_j^n + \nu \sum_{j=1}^{N-1} U_{j+1}^n + \nu \sum_{j=1}^{N-1} U_{j-1}^n + \frac{1}{2}U_N^n - \nu U_N^n + \nu U_{N-1}^n \\
=&(\frac{1}{2}U_0^n + \sum_{j=1}^{N-1} U_j^n + \frac{1}{2}U_N^n) - \nu U_0^n + \nu U_1^n - 2\nu \sum_{j=1}^{N-1} U_j^n + \nu \sum_{j=2}^{N} U_j^n + \nu \sum_{j=0}^{N-2} U_j^n - \nu U_N^n + \nu U_{N-1}^n \\
=&\sum_{j=0}^{N} U_j^n - \nu U_0^n + \nu U_1^n - \nu U_1^n + \nu U_N^n - \nu U_{N-1}^n + \nu U_0^n - \nu U_N^n + \nu U_{N-1}^n \\
=&\frac{1}{2}U_0^n + \sum_{j=1}^{N-1} U_j^n + \frac{1}{2}U_N^n
\end{aligned}
\tag{31}
$$

Therefore we have shown that the conservation principle holds for this discretization of the diffusion equation.

3.3 2D system

3.3.1 Discretization

Now that we have discussed diffusion in 1D, we can do the same thing for the 2D case.

First we need a 2D grid. We will use the index j for the x direction and k for the y direction, see figure 9. We assume that the domain is a rectangle.

We need to define discretizations for nine different cases. These are the bulk, the four edges and the four corners of the domain. We also define v_x and v_y as $\Delta t/(\Delta x)^2$ and $\Delta t/(\Delta y)^2$ respectively.

For the bulk, so $U_{j,k}$ with $j \neq 0, N$ and $k \neq 0, M$:

$$U^{n+1}_{j,k} = U^n_{j,k} + v_x(U^n_{j+1,k} - 2U^n_{j,k} + U^n_{j-1,k}) + v_y(U^n_{j,k+1} - 2U^n_{j,k} + U^n_{j,k-1}) \tag{32}$$

For the edges. we can use the ghost cell method to implement the boundary conditions. We can use the left edge as an example. $u_x = 0$ implies that

$$\frac{U^n_{-1,k} - U^n_{1,k}}{2\Delta x} = 0 \tag{33}$$

From this, we can conclude that $U^n_{-1,k} = U^n_{1,k}$ and therefore we can replace all the $U^n_{-1,k}$ in the regular scheme with $U^n_{1,k}$, just as we have done in 1D.

This means that for the left edge, so for $U_{0,k}$ with $k \neq 0, M$, we get

$$U^{n+1}_{0,k} = U^n_{0,k} + 2v_x(U^n_{1,k} - U^n_{0,k}) + v_y(U^n_{0,k+1} - 2U^n_{0,k} + U^n_{0,k-1}) \tag{34}$$

For the right edge, so for $U_{N,k}$ with $k \neq 0, M$, we get

$$U^{n+1}_{N,k} = U^n_{N,k} + 2v_x(U^n_{N-1,k} - U^n_{N,k}) + v_y(U^n_{N,k+1} - 2U^n_{N,k} + U^n_{N,k-1}) \tag{35}$$

For the bottom edge, $U_{j,0}$ with $j \neq 0, N$,

$$U^{n+1}_{j,0} = U^n_{j,0} + v_x(U^n_{j+1,0} - 2U^n_{j,0} + U^n_{j-1,0}) + 2v_y(U^n_{j,1} - U^n_{j,0}) \tag{36}$$

Lastly for the top edge, $U_{j,M}$ with $j \neq 0, N$,

$$U^{n+1}_{j,M} = U^n_{j,M} + v_x(U^n_{j+1,M} - 2U^n_{j,M} + U^n_{j-1,M}) + 2v_y(U^n_{j,M-1} - U^n_{j,M}) \tag{37}$$

Next we will look at the equations for the four corners.
The bottom left corner:

$$U^{n+1}_{0,0} = U^n_{0,0} + 2v_x(U^n_{1,0} - U^n_{0,0}) + 2v_y(U^n_{0,1} - U^n_{0,0}) \tag{38}$$

The bottom right corner:

$$U^{n+1}_{N,0} = U^n_{N,0} + 2v_x(U^n_{N-1,0} - U^n_{N,0}) + 2v_y(U^n_{N,1} - U^n_{N,0}) \tag{39}$$

The top left corner:

$$U^{n+1}_{0,M} = U^n_{0,M} + 2v_x(U^n_{1,M} - U^n_{0,M}) + 2v_y(U^n_{0,M-1} - U^n_{0,M}) \tag{40}$$

The top right corner:

$$U^{n+1}_{N,M} = U^n_{N,M} + 2v_x(U^n_{N-1,M} - U^n_{N,M}) + 2v_y(U^n_{N,M-1} - U^n_{N,M}) \tag{41}$$

3.3.2 Conservation

Now that we have the equations, we can look at how to show the conservation. Define

$$A^n = \sum_{k=1}^{M-1}\sum_{j=1}^{N-1} U^n_{j,k} + \frac{1}{2}\left(\sum_{k=1}^{M-1} U^n_{0,k} + \sum_{k=1}^{M-1} U^n_{N,k} + \sum_{j=1}^{N-1} U^n_{j,0} + \sum_{j=1}^{N-1} U^n_{j,M}\right) + \frac{1}{4}\left(U^n_{0,0} + U^n_{N,0} + U^n_{0,M} + U^n_{N,M}\right) \tag{42}$$

Then quantity U is conserved when

$$A^{n+1} = A^n \tag{43}$$

By the same argument that we used in the section about conservation in 1D, the contribution of the edges is $\frac{1}{2}$ and the contributions of the corners is $\frac{1}{4}$.

The next step to show conservation is to substitute the discretizations of all parts in A^{n+1}. We will first consider the terms that are not a product of ν and U.

Adding up all the terms that do not have a ν in them gives

$$\sum_{k=1}^{M-1}\sum_{j=1}^{N-1} U^n_{j,k} + \frac{1}{2}\left(\sum_{k=1}^{M-1} U^n_{0,k} + \sum_{k=1}^{M-1} U^n_{N,k} + \sum_{j=1}^{N-1} U^n_{j,0} + \sum_{j=1}^{N-1} U^n_{j,M}\right) + \frac{1}{4}\left(U^n_{0,0} + U^n_{N,0} + U^n_{0,M} + U^n_{N,M}\right) \tag{44}$$

which is exactly A^n.

This means that

$$A^{n+1} = A^n + C \tag{45}$$

Where C is defined as the terms that do have a product of ν and U after substitution of the discretizations in A^{n+1}. Our goal is to show that C is equal to zero, because then we can conclude that U must be conserved. As a sanity check, we can let Δt go to zero, so we approach the continuous case. Then ν goes to zero and that means that C as a whole goes to zero. We see that in that case we indeed have conservation.

To evaluate the case numerical case where ν does not equal zero, we will consider the bulk, edges and corners in C separately and join the results periodically.

The bulk We will look at the contributions to C from the bulk first.

$$\sum_{k=1}^{M-1}\sum_{j=1}^{N-1}\left[\nu_x(U^n_{j+1,k} - 2U^n_{j,k} + U^n_{j-1,k}) + \nu_y(U^n_{j,k+1} - 2U^n_{j,k} + U^n_{j,k-1})\right] \tag{46}$$

The double sum can be split in two, since they are finite sums.

$$\sum_{k=1}^{M-1}\sum_{j=1}^{N-1}\nu_x(U^n_{j+1,k} - 2U^n_{j,k} + U^n_{j-1,k}) + \sum_{k=1}^{M-1}\sum_{j=1}^{N-1}\nu_y(U^n_{j,k+1} - 2U^n_{j,k} + U^n_{j,k-1}) \tag{47}$$

We will look at the left double sum of (47) first. We can change the sum in the following way.

$$\nu_x \sum_{k=1}^{M-1} \left(\sum_{j=2}^{N} U^n_{j,k} - 2 \sum_{j=1}^{N-1} U^n_{j,k} + \sum_{j=0}^{N-2} U^n_{j,k} \right) \tag{48}$$

After carefully looking at which terms cancel, we find that the following is left over.

$$\nu_x \sum_{k=1}^{M-1} \left(U^n_{N,k} + U^n_{0,k} - U^n_{N-1,k} - U^n_{1,0} \right) \tag{49}$$

Similarly we can rewrite the right sum of equation (47).

$$\nu_y \sum_{j=1}^{N-1} \left(\sum_{k=2}^{M} U^n_{j,k} + \sum_{k=1}^{M-1} U^n_{j,k} + \sum_{k=0}^{M-2} U^n_{j,k} \right) \tag{50}$$

The terms that are left over are

$$\nu_y \sum_{j=1}^{N-1} \left(U^n_{j,M} + U^n_{j,0} - U^n_{j,M-1} - U^n_{j,1} \right) \tag{51}$$

We conclude that from the contributions to C from the bulk, the terms that are left over are the sum of equations (49) and (51).

Left edge Now we look at the contributions to C from the edges and see what will be left over. The terms for the left edge are

$$\frac{1}{2} \sum_{k=1}^{M-1} \left[2\nu_x \left(U^n_{1,k} - U^n_{0,k} \right) + \nu_y \left(U^n_{0,k+1} - 2U^n_{0,k} + U^n_{0,k-1} \right) \right] \tag{52}$$

We split up the sum and change the indices.

$$\nu_x \sum_{k=1}^{M-1} \left(U^n_{1,k} - U^n_{0,k} \right) + \frac{1}{2}\nu_y \left(\sum_{k=2}^{M} U^n_{0,k} - 2 \sum_{k=1}^{M-1} U^n_{0,k} + \sum_{k=0}^{M-2} U^n_{0,k} \right) \tag{53}$$

After removing all the terms that cancel each other, we are left with

$$\nu_x \sum_{k=1}^{M-1} \left(U^n_{1,k} - U^n_{0,k} \right) + \frac{1}{2}\nu_y \left(U^n_{0,0} + U^n_{0,M} - U^n_{0,1} - U^n_{0,M-1} \right) \tag{54}$$

Right edge The terms of the right edge:

$$\frac{1}{2} \sum_{k=1}^{M-1} \left[2\nu_x \left(U^n_{N-1,k} - U^n_{N,k} \right) + \nu_y \left(U^n_{N,k+1} - 2U^n_{N,k} + U^n_{N,k-1} \right) \right] \tag{55}$$

We again split up the sum and change the indices.

$$\nu_x \sum_{k=1}^{M-1} \left(U^n_{N-1,k} - U^n_{N,k} \right) + \frac{1}{2}\nu_y \left(\sum_{k=2}^{M} U^n_{N,k} - 2 \sum_{k=1}^{M-1} U^n_{N,k} + \sum_{k=0}^{M-2} U^n_{N,k} \right) \tag{56}$$

The terms that are left are:

$$\nu_x \sum_{k=1}^{M-1} \left(U^n_{N-1,k} - U^n_{N,k} \right) + \frac{1}{2}\nu_y \left(U^n_{N,0} + U^n_{N,M} - U^n_{N,1} - U^n_{N,M-1} \right) \tag{57}$$

Bottom edge The contributing terms from the bottom edge are

$$\frac{1}{2} \sum_{j=1}^{N-1} \left[\nu_x \left(U^n_{j+1,0} - 2U^n_{j,0} + U^n_{j-1,0} \right) + 2\nu_y \left(U^n_{j,1} - U^n_{j,0} \right) \right] \tag{58}$$

We use the same strategy, namely splitting the sum and changing the indices.

$$\frac{1}{2}\nu_x \left(\sum_{j=2}^{N} U^n_{j,0} - 2 \sum_{j=1}^{N-1} U^n_{j,0} + \sum_{j=0}^{N-2} U^n_{j,0} \right) + \nu_y \sum_{j=1}^{N-1} \left(U^n_{j,1} - U^n_{j,0} \right) \tag{59}$$

Which means that the left over terms are

$$\frac{1}{2}\nu_x \left(U^n_{0,0} + U^n_{N,0} - U^n_{1,0} - U^n_{N-1,0} \right) + \nu_y \sum_{j=1}^{N-1} \left(U^n_{j,1} - U^n_{j,0} \right) \tag{60}$$

Top edge The terms that contribute to C from the top edge are

$$\frac{1}{2} \sum_{j=1}^{N-1} \left[\nu_x \left(U^n_{j+1,M} - 2U^n_{j,M} + U^n_{j-1,M} \right) + 2\nu_y \left(U^n_{j,M-1} - U^n_{j,M} \right) \right] \tag{61}$$

We can rewrite this as

$$\frac{1}{2}\nu_x \left(\sum_{j=2}^{N} U^n_{j,M} - 2 \sum_{j=1}^{N-1} U^n_{j,M} + \sum_{j=0}^{N-2} U^n_{j,M} \right) + \nu_y \sum_{j=1}^{N-1} \left(U^n_{j,M-1} - U^n_{j,M} \right) \tag{62}$$

Which means that the left over terms are

$$\frac{1}{2}\nu_x \left(U^n_{0,M} + U^n_{N,M} - U^n_{1,M} - U^n_{N-1,M} \right) + \nu_y \sum_{j=1}^{N-1} \left(U^n_{j,M-1} - U^n_{j,M} \right) \tag{63}$$

Combining 1

The next thing that we will do is add up all the terms that are left over from the bulk to the terms that are left over from the edges to see which ones cancel.

The combination of all leftover terms, which is the sum of equations (49), (51), (54), (57), (60) and (63), looks as follows:

$$
\begin{aligned}
&v_x \sum_{k=1}^{M-1} \left(U^n_{N,k} + U^n_{0,k} - U^n_{N-1,k} - U^n_{1,0}\right) + v_y \sum_{j=1}^{N-1} \left(U^n_{j,M} + U^n_{j,0} - U^n_{j,M-1} - U^n_{j,1}\right) \\
&+v_x \sum_{k=1}^{M-1} \left(U^n_{1,k} - U^n_{0,k}\right) + \frac{1}{2} v_y \left(U^n_{0,0} + U^n_{0,M} - U^n_{0,1} - U^n_{0,M-1}\right) \\
&+v_x \sum_{k=1}^{M-1} \left(U^n_{N-1,k} - U^n_{N,k}\right) + \frac{1}{2} v_y \left(U^n_{N,0} + U^n_{N,M} - U^n_{N,1} - U^n_{N,M-1}\right) \\
&+\frac{1}{2} v_x \left(U^n_{0,0} + U^n_{N,0} - U^n_{1,0} - U^n_{N-1,0}\right) + v_y \sum_{j=1}^{N-1} \left(U^n_{j,1} - U^n_{j,0}\right) \\
&+\frac{1}{2} v_x \left(U^n_{0,M} + U^n_{N,M} - U^n_{1,M} - U^n_{N-1,M}\right) + v_y \sum_{j=1}^{N-1} \left(U^n_{j,M-1} - U^n_{j,M}\right)
\end{aligned}
\tag{64}
$$

For every remaining term that came from the bulk, there exists a term that came from one of the edges that has the opposite sing, so the entirety of the remaining terms from the bulk is gone. The terms that are now left over are then

$$
\begin{aligned}
&\frac{1}{2} v_y \left(U^n_{0,0} + U^n_{0,M} - U^n_{0,1} - U^n_{0,M-1}\right) \\
&+\frac{1}{2} v_y \left(U^n_{N,0} + U^n_{N,M} - U^n_{N,1} - U^n_{N,M-1}\right) \\
&+\frac{1}{2} v_x \left(U^n_{0,0} + U^n_{N,0} - U^n_{1,0} - U^n_{N-1,0}\right) \\
&+\frac{1}{2} v_x \left(U^n_{0,M} + U^n_{N,M} - U^n_{1,M} - U^n_{N-1,M}\right)
\end{aligned}
\tag{65}
$$

The corners

All that is left is to add the terms that were left over from the corners to equation (65). We will first look at what the remaining terms from the corners are.

$$
\begin{aligned}
&\frac{1}{4} \left(2v_x \left(U^n_{1,0} - U^n_{0,0}\right) + 2v_y \left(U^n_{0,1} - U^n_{0,0}\right)\right) \\
&+\frac{1}{4} \left(2v_x \left(U^n_{N-1,0} - U^n_{N,0}\right) + 2v_y \left(U^n_{N,1} - U^n_{N,0}\right)\right) \\
&+\frac{1}{4} \left(2v_x \left(U^n_{1,M} - U^n_{0,M}\right) + 2v_y \left(U^n_{0,M-1} - U^n_{0,M}\right)\right) \\
&+\frac{1}{4} \left(2v_x \left(U^n_{N-1,M} - U^n_{N,M}\right) + 2v_y \left(U^n_{N,M-1} - U^n_{N,M}\right)\right)
\end{aligned}
\tag{66}
$$

This can be simplified to

$$\begin{aligned}
&\frac{1}{2}\nu_x\left(U^n_{1,0} - U^n_{0,0} + U^n_{N-1,0} - U^n_{N,0} + U^n_{1,M} - U^n_{0,M} + U^n_{N-1,M} - U^n_{N,M}\right) \\
&\frac{1}{2}\nu_y\left(U^n_{0,1} - U^n_{0,0} + U^n_{N,1} - U^n_{N,0} + U^n_{0,M-1} - U^n_{0,M} + U^n_{N,M-1} - U^n_{N,M}\right)
\end{aligned} \tag{67}$$

Combining 2

Now we add equations (65) and (67) up to each other and after some careful bookkeeping, the result is that each term in equation (65) is canceled by a term in equation (67).

We have shown that C in equation (45) is zero.
Therefore we have shown that equation (43) holds for the numerical method we will use and that means that we can accurately describe the diffusion in the 2D model.

3.4 Validation of numerical diffusion

We have seen that from a mathematics view, the discretizations are consistent with the physical background, but it is also important that the actual implementation also follows this consistency. Of course this can only be done within some given error margin.

To test the accuracy of the implementation, we look at grid refinement. One specific point is selected such that for every refinement, the point exists in our numerical grid. We have picked the point $(1/4, 1/4)$ together with the grid sizes $(N_x, N_y) = (2^k + 1, 2^k + 1)$ for $k = 3, 4, 5, 6$. For the length of the domain, we have chosen $L_x = L_y = 2$. Lastly, we have chosen Δt such that ν_x and ν_y are 0.25 for each grid size. The results of the test can be found in figure 10. The solutions are converging so the implementation works.

We have also tested the conservation numerically and verified that it works. Additionally, we computed the maximum value of the solution at every time step and we found that it decreases exponentially and converges to a steady state value, which indicates that the implementation works as intended.

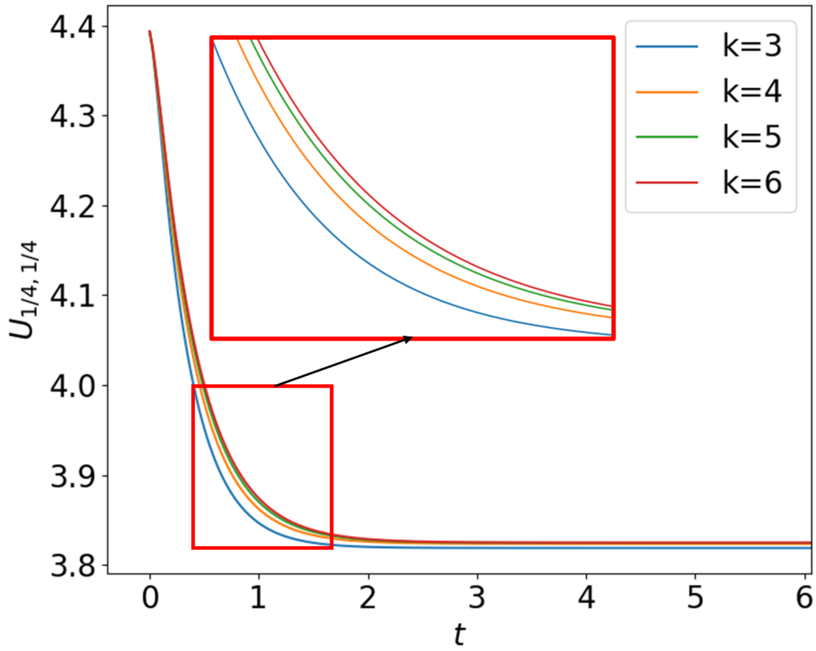

FIGURE 10: The computed solution over time of $U_{1/4,1/4}$ for $N_x = N_y = 2^k + 1$ grid points

4 Calculation of spin-galvanic effects in 2D

In this section we will look at how we are going to add the equations that describe the spin-galvanic effect to our numerical diffusion core. Then we will present the calculations made with the external magnetic field pointing in different directions. We will also show what the dependence on the strength of the magnetic field and the strength of the spin-galvanic effect. From now on we will use γ as the value of γ_{xy}. We do this to simplify the notation, since we only study the case with $\gamma_{xy} = -\gamma_{yx}$ and the rest of the values are zero.

4.1 Spin-galvanic effect in the numerical model

We have stated what the equations for the spin-galvanic effect are in section 2.3. Now we need to discretize the equations so we can add the equations to our diffusion core.

The addition of the spin-galvanic terms introduces a coupling between μ and all S^c, so we will need another discretized variable to the numerical scheme.

- $U^n_{j,k}$ is μ at position j, k in the grid and at time step n.
- $V^{c,n}_{j,k}$ is S^c, where c can be x, y or z, at position j, k and at time step n.

The cross-dependencies are first order derivatives and we can discretize the terms with central differencing, just like we have done with the boundary conditions in the diffusion core.

The boundary conditions have changed compared to the diffusion core, so we need to pay close attention to how we incorporate the boundaries in the numerical scheme. We want to make use of the ghost-cell method again.

4.2 Why there is a voltage in the steady state

With the spin-galvanic effect, applying a magnetic field causes electrons to move to one side of the material. The accumulation of electrons on one side and the absence of electrons on the other side of the material is then exactly the gradient in μ. This gradient is a voltage across the material and this voltage causes a current to flow in the opposite direction of the gradient. This means that we have two currents, each in the opposite direction. The steady state situation is formed when the current generated by the magnetic field is fully canceled out by the current caused by the voltage.

4.3 Calculation of dependency on the direction and strength of the magnetic field

In figures 11, 12 and 13, the voltages in the presence of the spin-galvanic effect are shown. The parameter values that we have used for these calculations can be found in table 1. As a reminder, we are interested in the case where $\gamma_{xy} = -\gamma_{yx}$ and the rest of the values for γ_{kl} is zero.

Just as we expected from our understanding of the spin-galvanic effect, applying a magnetic field will result in a gradient in μ. Furthermore, in figure 11 the magnetic field points in the x-direction and the result is a gradient in μ in the y-direction. Similarly, in figure 12 the magnetic field in the y-direction causes a gradient in the x-direction. In figure 13 the magnetic field is pointing in the positive x- and y-direction with the gradient in μ now being in the positive x-direction and negative y-direction. The gradient in μ is perpendicular to the magnetic field and that is exactly as it is supposed to be. This can be derived from equation (6). since he only terms in γ that are not zero are γ_{xy} and γ_{yx}.

The third property to mention is that the gradient should increase linearly if the strength of the spin-galvanic is increased. The confirmation can be found in figure 14 where we see that the maximum value of μ (and thus the gradient) is linear in γ.

The gradient does not only increase linearly with γ. When the time derivative of the magnetic field $\dot{B}$ is increased, the gradient in μ also increases linearly. From equation (7), when we look at the steady state and ignore the coupling with μ, the derivatives vanish and we get that S^c is linearly related to $\dot{B}$. Then we look at equation (6) and we see that μ is linearly related to S^c. It follows that μ will also increase linearly with an increase in $\dot{B}$. This is illustrated in figure 15.

Parameter	Parameter value		
	Figure 11	Figure 12	Figure 13
α	0	0	0
τ_{SO}	1	1	1
γ_{xy}	0.1	0.1	0.1
$(\chi \dot{B})^x$	1	0	$\frac{1}{2}\sqrt{2}$
$(\chi \dot{B})^y$	0	1	$\frac{1}{2}\sqrt{2}$
$(\chi \dot{B})^z$	0	0	0

TABLE 1: Parameters and the values that have been used to do the calculations of the voltages in all three situations

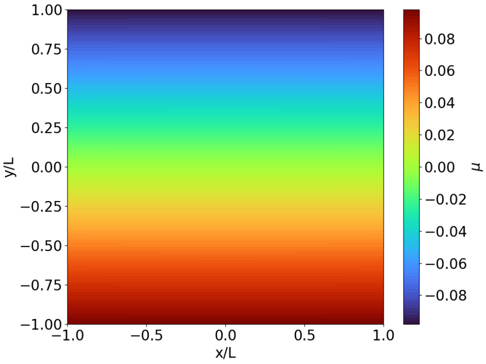

FIGURE 11: The steady state solution of μ generated by a magnetic field in the x-direction

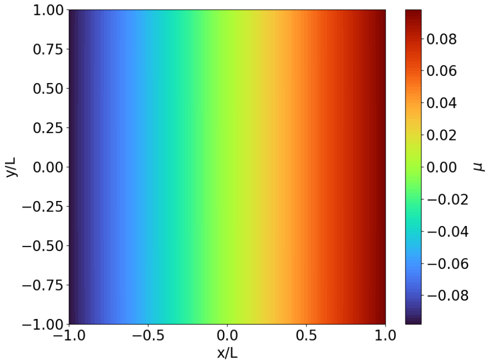

FIGURE 12: The steady state solution of μ generated by a magnetic field in the y-direction

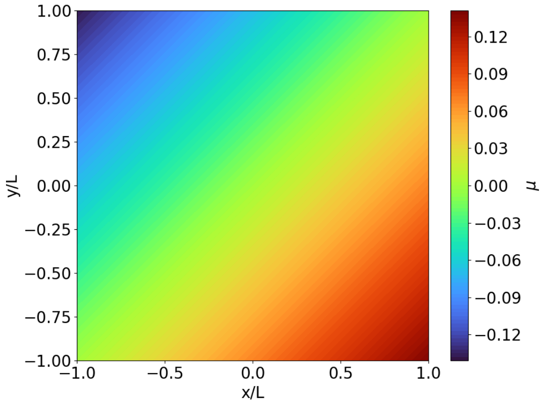

FIGURE 13: The steady state solution of μ generated by a magnetic field in the x- and y-direction

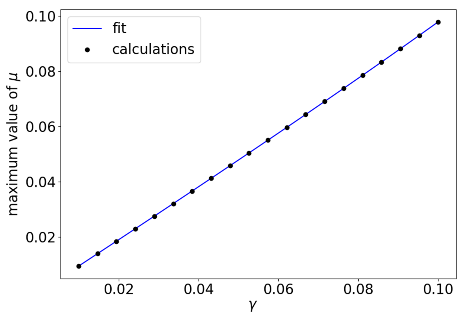

FIGURE 14: The maximum value of μ as a function of the strength of the spin galvanic effect

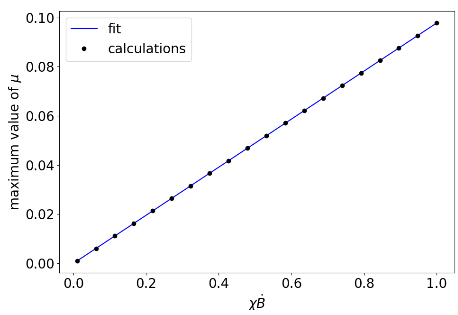

FIGURE 15: The maximum value of μ as a function of the strength of the magnetic field

4.4 Spin accumulations

For the implementation, we have ignored the terms of order γ^2 in the boundaries. We have made this choice because in practice, the spin-galvanic effect is often rather weak and then the values in γ are small.

First, we will take a look at the justification of not implementing the terms of order γ^2.

Figures 16 and 17 show some abnormal behaviour. The magnetic field was chosen such that it only points in the y-direction. We expect a gradient in S^x in the y-direction only, but we can see in the figures that we have a gradient in the x-direction as well. This gradient is caused by the boundary terms that are second order in γ that we have left out of the model. We can see that having γ at a value that is too large will cause the gradient in the x-direction. The difference between figures 16 and 17 is the strength of the spin-galvanic effect and we see that making γ twice as small results in the maximum value of S^x to get divided by 4, which is an indication of the effect being quadratic in γ. In figure 18, we can see that the effect is indeed quadratic in γ, which shows that the undesired behaviour is indeed caused by the absence of the boundary terms that are quadratic in γ.

S^y has a similar problem. Our calculations show that S^y is almost constant in the steady state, but there is also a gradient in the x-direction of order γ with corrections to S^y of order γ^2. The explanation can be again done by looking at equation (7) and (6). S^y is coupled to μ because a non-zero S^y generates a gradient of order γ in μ. The gradient in μ is on its own coupled back to S^y with a contribution of order γ. Together it means that we have corrections to S^y that are second order in γ.

The steady state calculation of S^z does not have that problem. S^z ends up at zero everywhere in the steady state, within a numerical error of 1×10^{-10}, which is the error that we have specified in our implementation. The components of the tensor γ that couple S^z to μ are all zero, so there is in fact no coupling at all. In equation (7) the coupling term then disappears entirely. In the steady state all the derivatives are zero and then it can be derived from the left over terms that $S^z = 0$ is the only solution, since the z component of the magnetic field is zero.

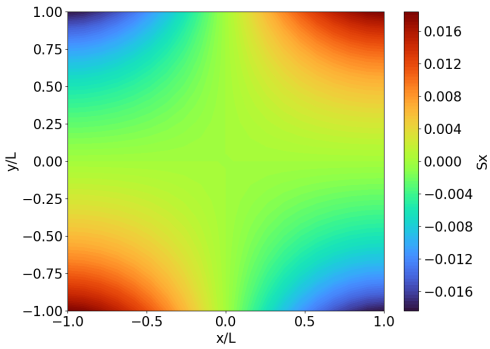

FIGURE 16: The steady state solution for S^x with $\gamma = 0.2$

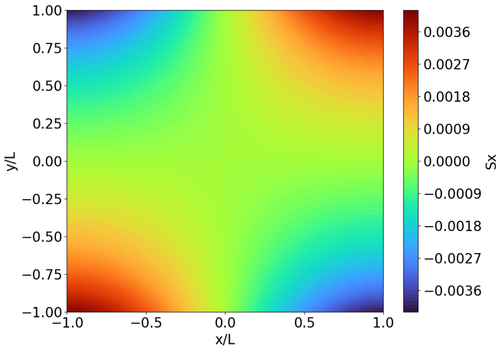

FIGURE 17: The steady state solution for S^x with $\gamma = 0.1$

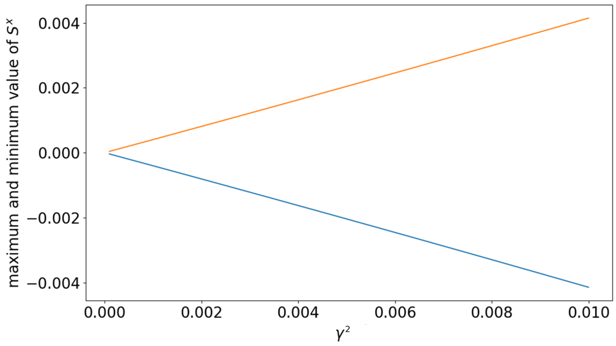

FIGURE 18: The maximum and minimum values of S^x as a function of the strength of the spin galvanic effect

5 Conclusion

We have calculated the spin-galvanic effect in a diffusive metal with spin-orbit coupling, specifically with Rashba spin-orbit coupling. We found that in the steady state there is a gradient in μ perpendicular to the direction of the applied magnetic field. We have calculated the first order effects in γ on μ.

There are some conditions to the choice of parameters and systems that apply when doing the calculations. The system that we look at have to be made from a certain type of material, namely a diffusive metal. The calculations do not work for systems such as semiconductors, because we assumed that the Fermi level is far away from the band gap. Also materials that are too clean, so materials that do not have many defects, can not be used in the calculations. This is because we have assumed that the energy associated to the scattering is larger than all other energies except for the Fermi energy. If we do not make the approximation that we have a lot of scattering, more computational power is needed. We also only look at the normal state, so superconductivity is not considered, which in most cases is a valid approximation. Because of the approximation that we have made in the boundary terms, the value for γ that we choose must be small enough.

Besides the calculations that we have done in this thesis, there are many other aspects of quantum transport in diffusive metals that can be considered. Implementing the boundary terms of order γ^2 will enable us to look at systems with stronger spin-orbit coupling. Additionally, other effects such as the spin-Hall effect [13] can be implemented, in combination with spin relaxation at the boundaries of the material, which will cause a local spin-galvanic effect. A long term plan can be the addition of superconductivity to the problem. The equations then become non-linear, but will give us some new insights.

References

[1] P. Taylor, enData growth worldwide 2010-2025 (2023).

[2] N. Zhang, Moore's Law is dead, long live Moore's Law! (2022), arXiv:2205.15011 [cs].

[3] B. Irfan, International Journal of Materials Science and Applications **10**, 94 (2021), number: 5 Publisher: Science Publishing Group.

[4] J. Puebla, J. Kim, K. Kondou, and Y. Otani, Communications Materials **1**, 1 (2020), publisher: Nature Publishing Group.

[5] E. I. Rashba, Journal of Superconductivity **18**, 137 (2005), arXiv:cond-mat/0408119.

[6] A. Manchon, H. C. Koo, J. Nitta, S. M. Frolov, and R. A. Duine, Nature Materials **14**, 871 (2015), publisher: Nature Publishing Group.

[7] K. D. Usadel, Physical Review Letters **25**, 507 (1970), publisher: American Physical Society.

[8] T. Kokkeler, F. S. Bergeret, and I. Tokatly, A universal phenomenology of charge-spin interconversion and dynamics in diffusive systems with spin-orbit coupling (2024), arXiv:2405.06334 [cond-mat].

[9] S. D. Ganichev, E. L. Ivchenko, V. V. Bel'kov, S. A. Tarasenko, M. Sollinger, D. Weiss, W. Wegscheider, and W. Prettl, Nature **417**, 153 (2002), publisher: Nature Publishing Group.

[10] W. Belzig, F. K. Wilhelm, C. Bruder, G. Schön, and A. D. Zaikin, Superlattices and Microstructures **25**, 1251 (1999), arXiv:cond-mat/9812297.

[11] W. Pauli, Zeitschrift fur Physik **43**, 601 (1927), publisher: Springer ADS Bibcode: 1927ZPhy...43..601P.

[12] B. J. Geurts, Lecture notes Numerical Methods for Partial Differential Equations (2023).

[13] J. Sinova, S. O. Valenzuela, J. Wunderlich, C. Back, and T. Jungwirth, Reviews of Modern Physics **87**, 1213 (2015), publisher: American Physical Society.